

BONE DISPLACEMENT INDUCED BY
AN APPLIED VOLTAGE

THESIS

Presented to the Graduate Council of
Southwest Texas State University
in Partial Fulfillment of
the Requirements

For the Degree of

MASTER OF SCIENCE

By

Mark J, VanElls, B.S.
San Marcos, Texas "

August, 1978

TABLE OF CONTENTS

LIST OF FIGURES iv

LIST OF TABLES v

ACKNOWLEDGMENTS vi

Chapter

I. INTRODUCTION 1

II. EXPERIMENTAL DESIGN 6

Bone Sample Preparation 6

Holographic Arrangement 8

Holographic Analysis 11

Experimental Procedure 13

III. EXPERIMENTAL RESULTS 16

IV. CONCLUSIONS 28

APPENDIX 30

REFERENCES 42

LIST OF FIGURES

Figure

1	An Illustration of Electrode Placement on a Tibia Mounted on a Vise	7
2	Arrangement of Laser and Components	9
3	Points of Observation where Observer is Normal to Hologram Plate	12
4	Geometrical Layout for Observations	14
5	Photographs of Reconstructed Double Exposure Holograms of an Adult Rat Tibia	17
6	Photographs of Reconstructed Double Exposure Holograms of a Juvenile Rat Tibia	18

LIST OF TABLES

Table

1	Data for Calculated Displacement of Adult Bone Surface	19
2	Data for Calculated Displacement of Juvenile Bone Surface	20
3a	Unit Vector Components of Adult Bone Surface	23
3b	Unit Vector Components of Juvenile Bone Surface	23
4	Calculated Data for Displacement of Adult Bone Surface	24
5	Calculated Data for Displacement of Juvenile Bone Surface	25
6	Average Values for Adult and Juvenile Bone Displacement	26

ACKNOWLEDGMENTS

Gratitude and appreciation are expressed to Dr. Caroline P. Benjamin for her valuable encouragement, advice, and support which she extended to me throughout my graduate studies and for her assistance in the preparation of this thesis. Appreciation is also extended to Dr. James R. Crawford for his patience and contributions to experimental technique and interpretation of results. In addition, I would like to thank Dr. Charles R. Willms for his comments and review of this thesis.

Mark J. VanElls

August, 1978

San Marcos, Texas

CHAPTER I

INTRODUCTION

Bone is a complex connective tissue comprising the skeletal system of most vertebrates. As is the case with other tissues, the physiological responses of bone are constantly being altered or regulated by bioelectric potentials. These potentials transmit environmental stimuli to bone which, in turn, responds to these stimuli within the limitations of its inherent genetic program. Since collagenous tissues such as cartilage, tendon, and bone continually generate strain-related potentials, these tissues can modify their architecture in response to the mechanical load (Williams, 1974; Bassett, 1968). The ability of live bone to remodel its architecture in order to meet functional demands was recognized as early as 1892 by J. Wolff. The nature of the response to the mechanical load normally is such that in any given bone osteoporosis and osteogenesis will occur simultaneously in different regions of the bone. These kinds of physiological activities can be determined by examining the internal and/or external structure of bone as well as by observing processes such as bone development, mineralization, growth, resorption, and repair. When a bone is examined in this manner, it is evident that

the overall effect of strain-related potentials generated by mechanical usage is to modify the architecture and pattern of bone growth. Hence, it can be stated that the physiological responses and morphology of bone reflect its mechanical usage, anatomical function, and state of maturity.

Bone tissue is mainly composed of an interstitial calcified organic matrix in which mature bone cells called osteocytes are imbedded. Primitive cells called osteoblasts regulate bone formation, alignment, and calcification initially by secreting this organic matrix around themselves. Minerals such as calcium phosphate and calcium carbonate are deposited secondarily in this organic matrix as hydroxyapatite crystals. The organic components render bone elastic and resilient, while the inorganic minerals make it hard. The organic matrix accounts for 38% of the dry bone weight and is composed mainly of collagen fibers. In addition there is a mucopolysaccharide called chondroitin sulfate (ground substance) which adheres to the collagen fibers. Although the physiological role of the ground substance is unknown, it is postulated that it assists in the calcification of collagen (Ham, 1961). It is the arrangement of the collagen fibers within the organic matrix which determines the ultimate shape of bone (Ham, 1961).

Bone tissue may be either mature or immature dependent on its state of development or according to its

location in an adult bone. Small amounts of immature bone are observed in most mature bones since the latter are being remodeled constantly by osteoporosis and osteogenesis. Fetal and young juvenile bones are called immature because they consist of proportionately more collagen and less ground substance and minerals than adult bones; consequently, the former are softer and more pliable than the latter. Furthermore, the organic matrix of immature bone is characterized by thick bundles of fine collagen fibrils which are arranged in a woven or interlaced pattern. As the bone matures, these fibrils will become rearranged into an organized system of fibrils in parallel array (Ham, 1961).

One bioelectric effect observed in both living and dead bone is piezoelectricity (the generation of an electrical polarization by a substance in response to mechanical stress). In 1957 Fukada and Yasuda discovered that bone exhibited an electrical polarization while mechanically deformed. Namely, a positive charge was formed on the convex side of the bent bone and a negative charge was formed on the concave side. Fukada and Yasuda (1964) later observed the converse piezoelectric effect; the bone became deformed when an electric field was applied. The following conclusions were drawn from these studies:

- 1) the organic matrix of bone transforms mechanical stress into an electric field (the piezoelectric effect); 2) when an applied electrical stimulus perturbs the matrix, bone

deformation results (the converse piezoelectric effect); 3) when mechanical stress is removed from a bone, the original polarity is restored; 4) when an electrical stimulus is removed from a bone, the original position of the bone is resumed. Although the precise origin and nature of the piezoelectric effect in bone is unknown, it has been observed that the presence of collagen in the matrix is essential for the piezoelectric response, (Williams, 1974).

Bassett et al., (1964) proposed that mechanical forces influence bone architecture by producing electrical signals in the organic matrix; these signals then stimulate bone remodeling. In vivo experiments have confirmed Bassett's work and have demonstrated that electrical stimulation can modify bone morphology. Namely, when voltage is applied to an undeformed bone, osteogenesis occurs at the cathode while osteoporosis is observed at the anode (Bourne, 1971). Furthermore, weak electrical currents on the order of microamperes have been used to repair fractures, to control disuse resorption, and to initiate bone growth (Williams, 1972; Harris, 1977). There is even a change observed in osteocyte cAMP levels which corresponds to electrical and mechanical perturbation preceding bone remodeling (Norton, 1977).

Castillo (1974) and White (1976) employed holographic interferometry as an experimental technique to measure bone displacement induced by an applied voltage.

With this technique it is possible to observe and measure small changes in an object's position. Castillo demonstrated that dried bone responds to an applied voltage in a dose-dependent manner; that is, an increase in voltage corresponded to an increase in bone displacement. The change in position of the bone's surface in response to stimulation was attributed to the converse piezoelectric nature of bone. The surface displacement of bone occurred immediately upon stimulation; moreover, displacement increased with time. It also was observed that following short intervals of electrical stimulation, the bone returned to its original position (White, 1976).

In the study described herein, freshly excised adult and juvenile rat tibiae were electrically stimulated at various voltages; concomitantly, the direction and magnitude of displacement were measured. Since adult and juvenile bones are morphologically and physiologically distinct, any differences observed in their displacement values could then be attributed to differences in the ability of their organic matrices to elicit the piezoelectric response.

CHAPTER II

EXPERIMENTAL DESIGN

Bone Sample Preparation

Bone samples were obtained from five adult female and five female juvenile white laboratory rats using the following procedure: animals were sacrificed individually by nembutol overdose; the left tibia was removed surgically; ligaments, tendons, and periosteum were removed from the shaft and epiphysis of the tibia proximal to the knee joint; the surface of the bone was cleansed gently with physiological saline and dried with an absorbent tissue. Immediately after the bone sample had been prepared, electroconductant (EKG) paste was applied to the area of electrode attachment to insure bone-electrode contact and two copper electrodes were looped around the transverse axis of the tibia at the junction between the epiphysis and shaft. The electrodes were placed 5 to 6 mm apart and were connected to a voltage-variable power source in such a way that the anode was proximal to the epiphysis. The foot and distal end of the tibia were mounted in a vise, fixing it in position but leaving the proximal end of the bone free to move (Figure 1). Moreover, since this experiment was designed to measure bone deformation in fresh bone, all

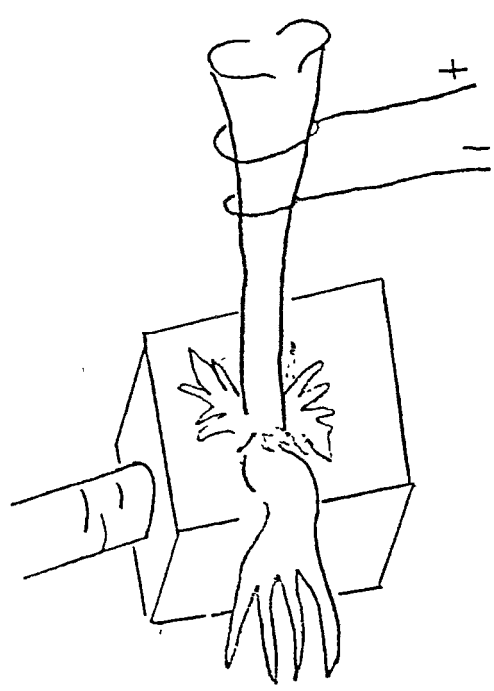


Figure 1. An illustration of electrode placement on a tibia mounted on a vise.

samples were secured, processed, electrically stimulated, and holographed within one hour after the animal's death.

Holographic Arrangement

A hologram of an object is formed by the superposition of two wavefronts on photographic film. The light used to record a hologram must be both coherent and monochromatic in order that high contrast interference fringes can be formed in a photographic emulsion. A laser is used as a light source since the light is monochromatic and coherent. A hologram is made by splitting a laser beam into an object beam and a reference beam. The object beam illuminates the object and the reference beam illuminates the film. Light that is scattered from the object interferes with the reference beam's coherent wavefront. The two fronts, object and reference, are combined at the photographic film plane. The superposition of the two beams results in a fringe pattern which is recorded on the photographic film, thus producing a hologram. Illumination of the processed hologram with the original reference beam gives a reconstructed wavefront as if it had come from the original object. The observer of the reconstructed wavefronts sees an object in a true three-dimensional form, complete with parallax and field depth (Cathey, 1974).

The experimental components for the holographic arrangement are seen in Figure 2. These components are a 15 milliwatt helium-neon laser, an electronic shutter, a

----- OBJECT BEAM
———— REFERENCE BEAM
M—MIRROR

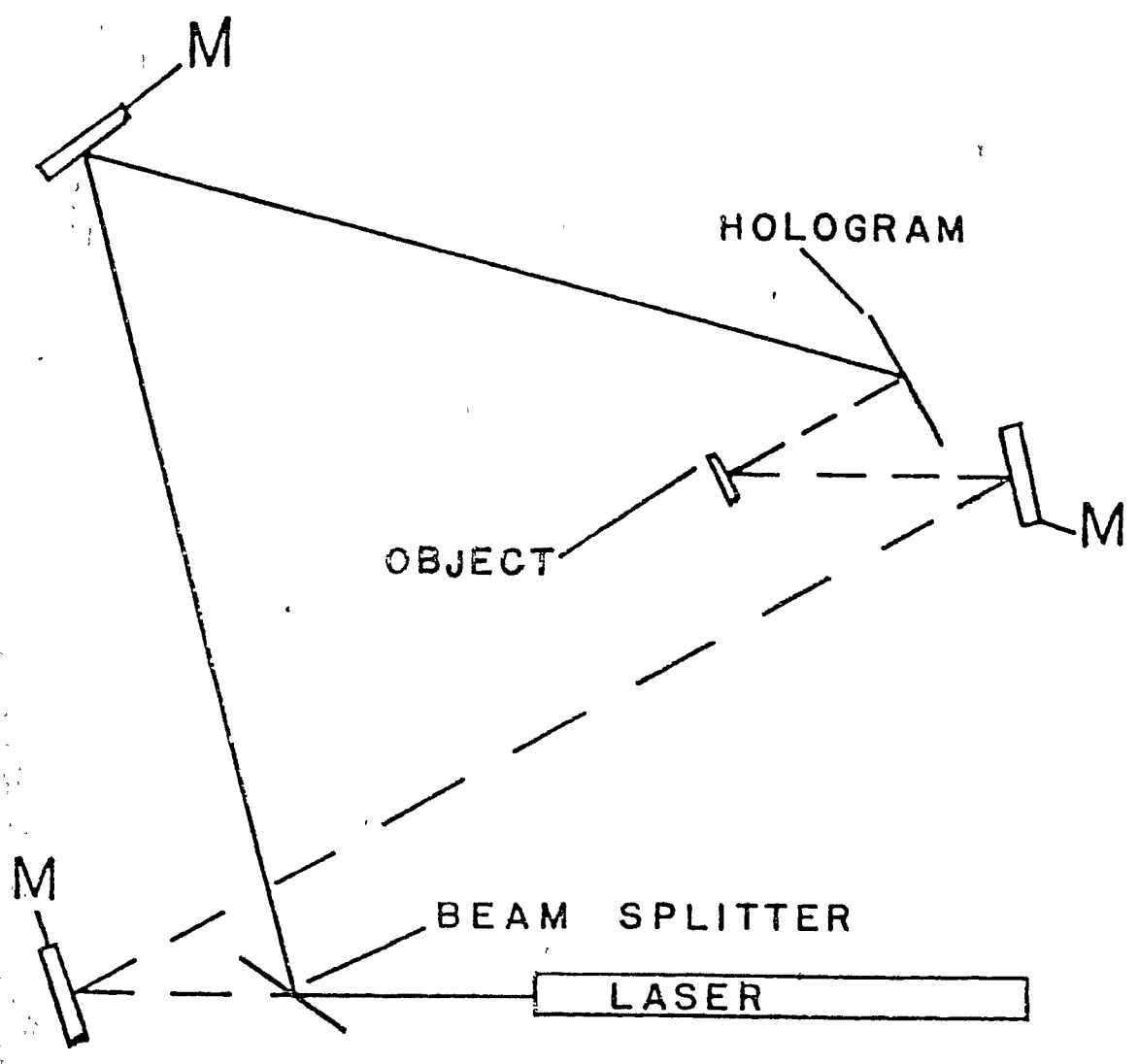


Figure 2. Arrangement of laser and components. This illustration is for clarification of the basic arrangement used for the proposed experiment. Components involved are: helium neon laser, a vibration isolation table, two spatial filters, one beam splitter, three front surface mirrors to direct the beam where desired, specimen table, and hologram plate.

variable beam splitter, three front surface mirrors, and two spatial filters. These components are fixed to a steel vibration isolation table. Photographic film plates are used to record the hologram. Each film plate is developed following the double exposure of the object (bone) and the film. The optical path length of the object and reference beams are kept as equal as possible. This is not a necessary condition as long as the difference is less than or equal to the coherent length of the laser; namely, approximately 20 centimeters.

In the experiments performed here, the tibia was placed 10 centimeters from the film. For the juvenile samples a biconvex lens was placed in front of the tibia to enlarge the image on the reconstructed hologram (exposures were made as described in "Experimental Procedure"). The photographic emulsion used was Agfa-Gevaert 10E75 on 4" X 5" glass plate with an anti-halation backing. The film was mounted securely in place in a film holder in a dark room just prior to exposure. Agfa-Gevaert 10E75 film plates were developed by placing them in Kodak D-19 developer for 5 minutes, a stop bath for 30 seconds, and Kodak Rapid Fixer with hardener for 5 minutes. After completing this process the plates were washed for 10 minutes in running water and air-dried.

Holographic Analysis

Double exposure holographic interferometry was the experimental method used to obtain measurements of bone deformation. Essentially this method consists of recording two successive holographic exposures on the same film of an object in two different positions. The first exposure is recorded, then stress is applied to the object. A second exposure is then taken on the same film. A reconstruction of the hologram shows two wavefronts of the object each having a distinct optical path. Dark interference lines which cross the surface of the reconstructed object result from a change in the object's wavefront between exposures. The fringe lines represent a change in position of the object between the first and second exposure. If the angle of observation is changed while the hologram is viewed, the location of the interference lines changes with respect to the observer. The fringe lines seen can be related to the displacement of the object between the two exposures.

Aleksandrov and Bonch-Bruevich (1967) developed a procedure for interpretation of the fringe patterns observed on a doubly-exposed hologram. This process involves observing the direction and number of fringes crossing a surface point on the bone. Fringe movement can be estimated to within approximately two-tenths of the width of a fringe. The points of observation used in this experiment are seen in Figure 3. The direction of fringe motion is assigned positive and negative values with respect to

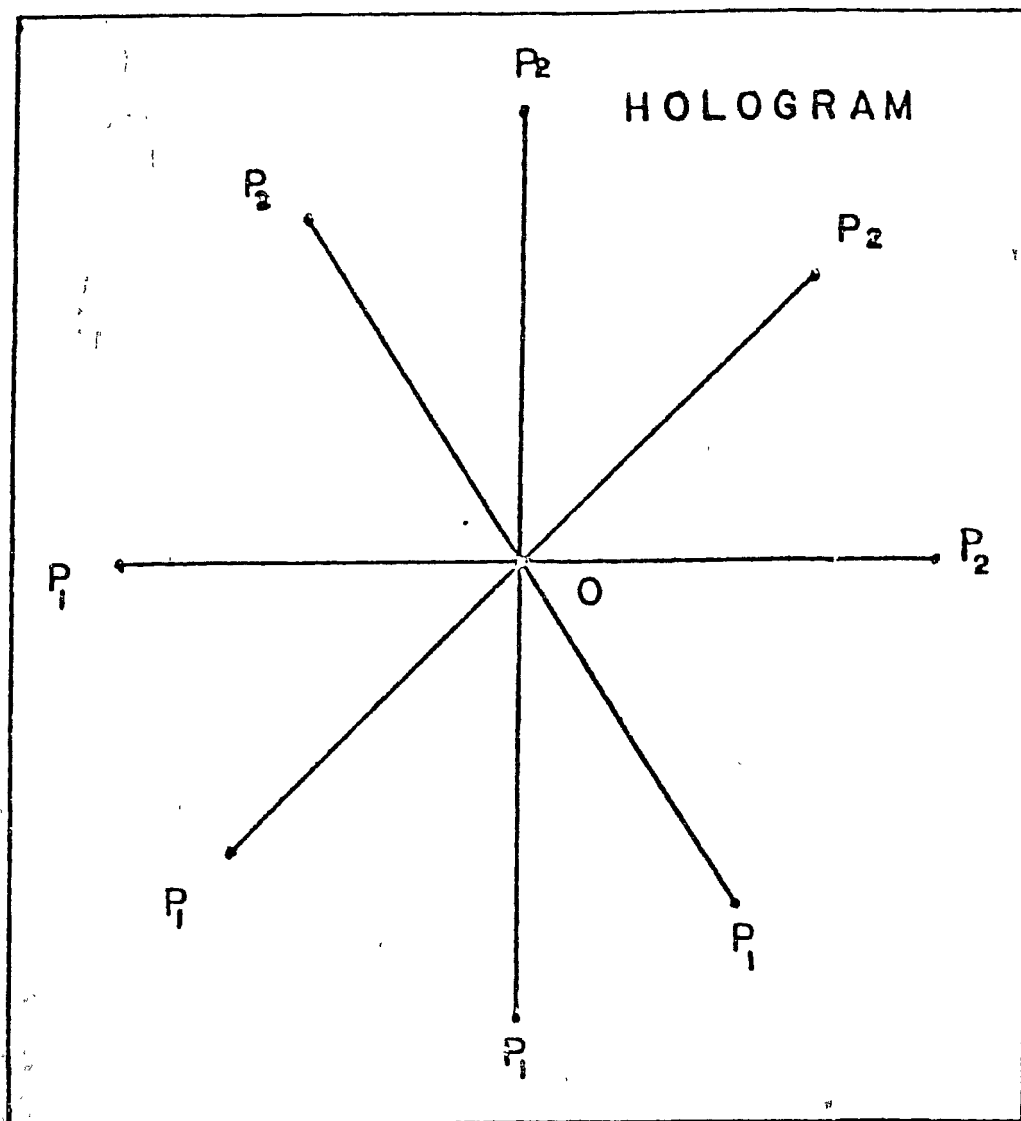


Figure 3. Points of observation where observer is normal to hologram plate. This illustration points out a sequence of four observations in the plane of the hologram plate. Each observation, from P_1 to P_2 , passes through the origin, O .

the observer's frame of reference P_1 to P_2 . The geometrical layout of the object and hologram coordinates for a particular point on the object's surface are seen in Figure 4. A mathematical and geometrical interpretation of the vectors seen in Figure 4 were discussed in detail by Castillo (1974) and White (1976). A computer program was used to determine the magnitude and direction of bone displacement (see Appendix I).

Experimental Procedure

A series of four double exposure holograms were made of each sample: the first hologram served as a control with no voltage applied; the second, third and fourth holograms were made in sequential voltage order from lowest to highest. Double exposure holograms were made of adult tibias when subjected to 100, 150, and 200 volts, while juvenile tibias were subjected to 15, 30, and 50 volts. Preliminary experiments revealed that the fringe patterns were consistent for the voltage increment applied when the samples were electrically stimulated prior to the first exposure. The period of electrical stimulation was 30 seconds for the adult samples and 20 seconds for the juvenile samples. Stimulation times of 20 seconds at 15 v and 30 seconds at 100 v were necessary to produce a detectable displacement in the juvenile and adult samples, respectively. Immediately following stimulation the first exposure was made and the electrodes were shorted. A

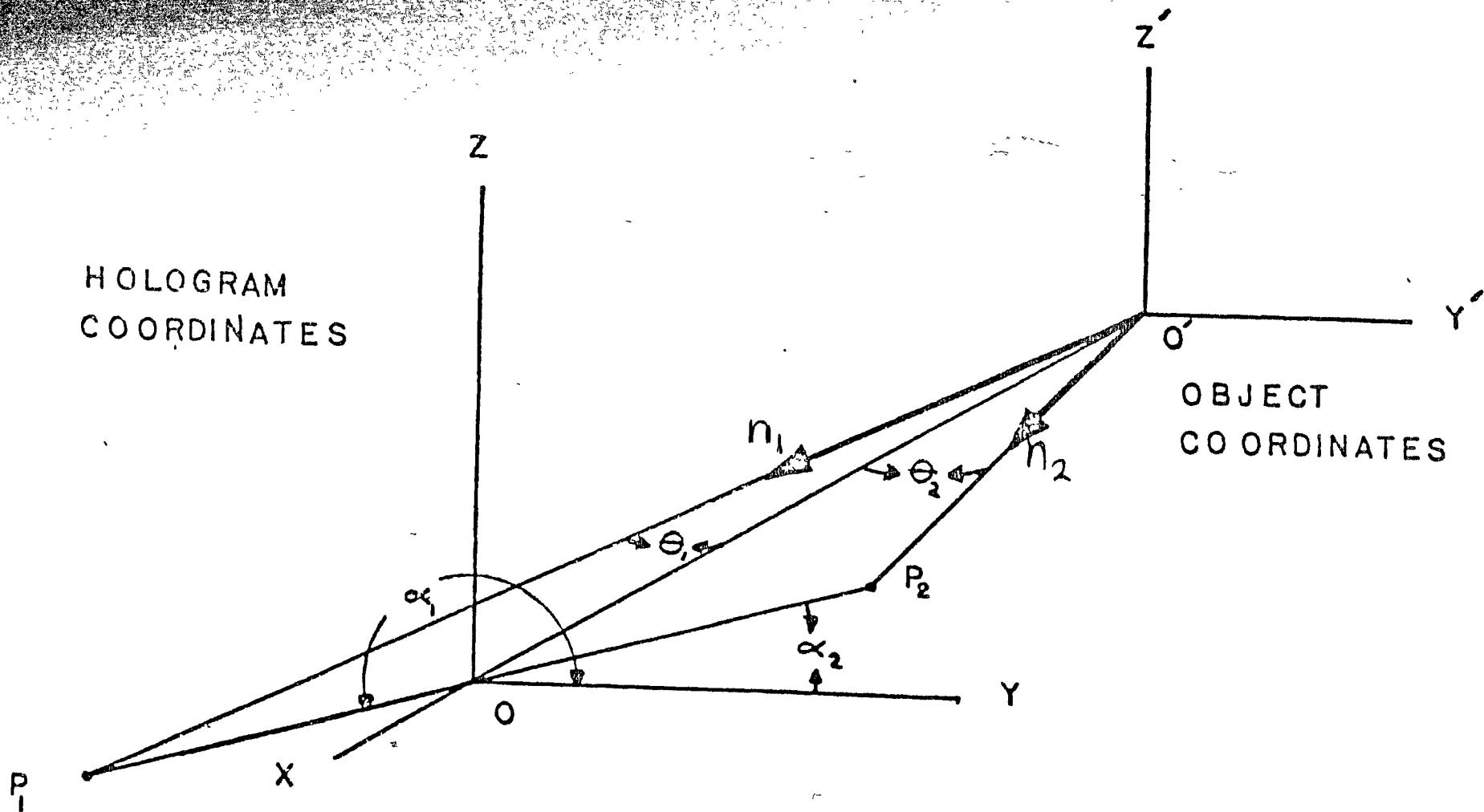


Figure 4. Geometrical layout for observations. The origin O' is located at the point of interest on the image of the particular surface. The origin O is located in the plane of the hologram by the intersection x' with that plane. The point O' is observed from the direction $O'P_1$ to $O'P_2$ with the number of fringe shifts counted while going from the direction $O'P_1$ to $O'P_2$. The unit vectors n_1 and n_2 are to be resolved into their components along the x , y , and z directions in terms of the angles θ_1 , θ_2 , α_1 , and α_2 .

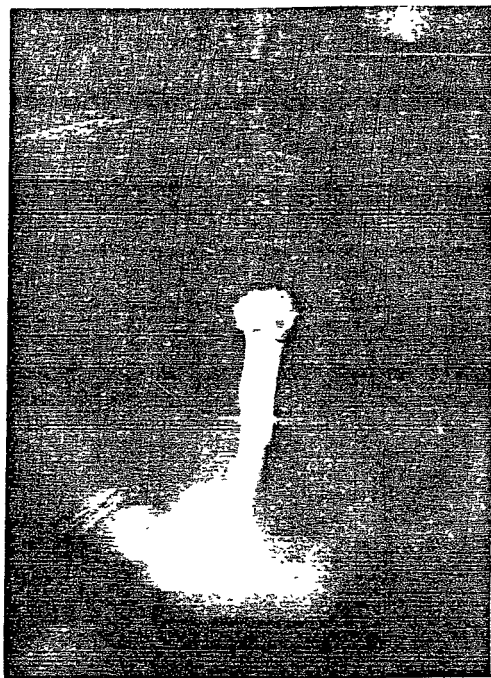
second exposure was made 30 seconds after the first exposure with the electrodes shorted for all samples. Thus, the adult samples had a longer stimulation time at higher voltages than the juvenile samples. After the voltage was applied to a sample a seven minute period elapsed with the electrodes shorted. This procedure insured that the surface of the bone returned to its initial position before proceeding to the next voltage increment.

In order to determine the direction of bone displacement a double exposure hologram was made of a plastic bar mounted on a micrometer. Between the first and second exposures a 20 micron displacement away from the film plate was made. The direction of fringe motion on the plastic bar served as a reference to determine the true direction of bone displacement.

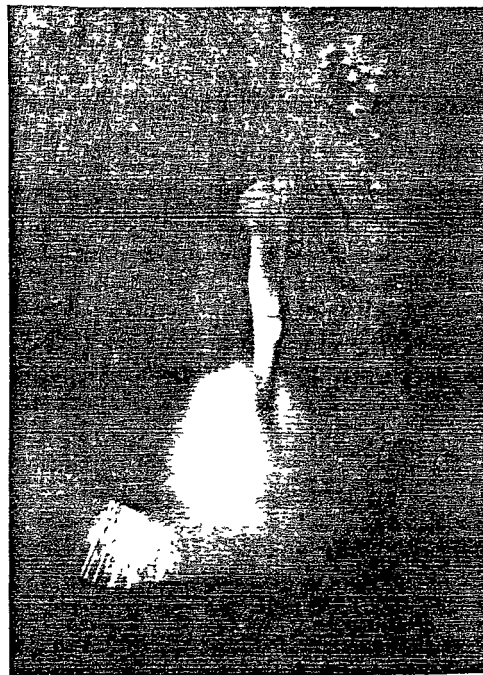
CHAPTER III

EXPERIMENTAL RESULTS

Double exposure holograms that were reconstructed exhibited interference fringes when the bone sample was subjected to an applied voltage (Figures 5 and 6). Control bone samples which were not electrically stimulated had no fringe patterns, indicating no bone displacement occurred as a result of either mounting the sample into the vise or of the attachment of the electrodes. As indicated in Figures 5 and 6, interference fringes were few in number and had a large band width in the juvenile and adult samples which were stimulated with low voltages (15 v and 100 v, respectively). Such fringes indicate a small change in the position of the bone surface. On the other hand, samples stimulated with the highest voltage increments (50 v in juvenile and 200 v in adult samples) exhibited numerous fringe lines with a narrow band width, indicating a greater displacement than occurred at the lower voltages. As expected, the application of voltages at the intermediate level (30 v in juvenile and 150 v in adult samples) resulted in an intermediate band width when compared to low and high voltage classes. Tables 1 and 2 are records of the number of fringes that passed through the point



A



B



C

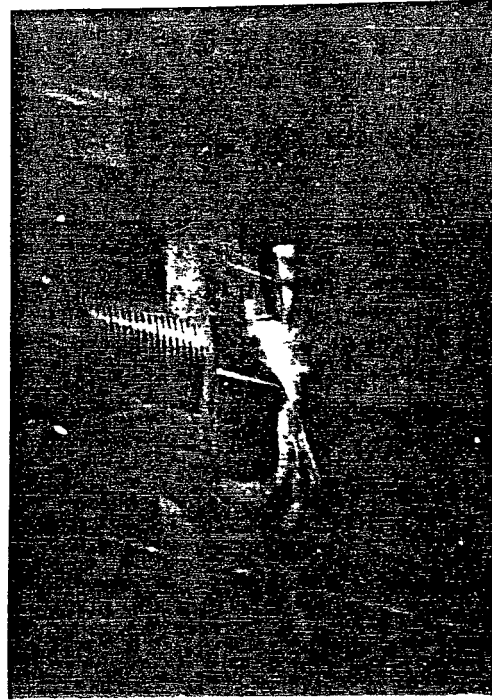


D

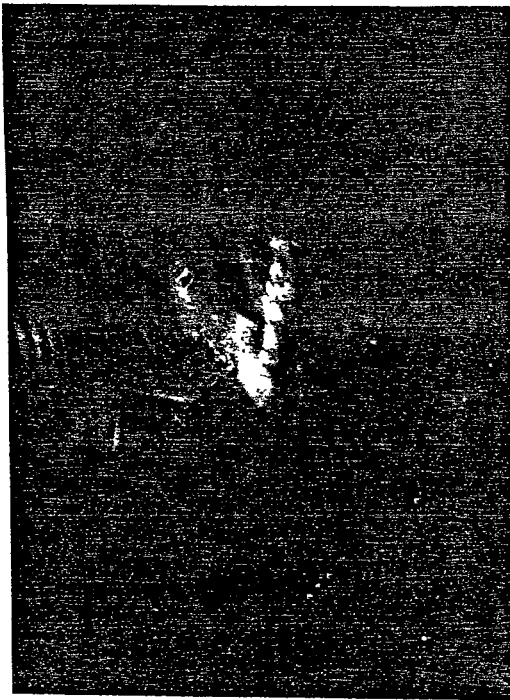
Figure 5. Photographs of reconstructed double exposure holograms of an adult rat tibia. The bone seen in A was a control with no voltage applied. Photographs B, C, and D show a bone stimulated with 100 v, 150 v, and 200 v respectively.



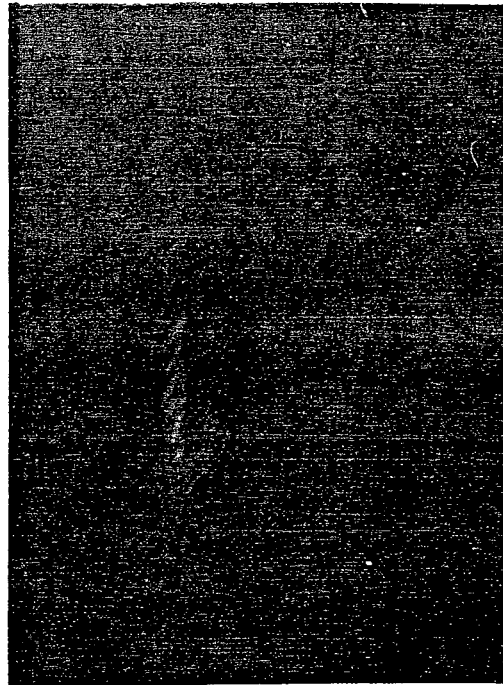
A



B



C



D

Figure 6. Photographs of reconstructed double exposure holograms of a juvenile rat tibia. The bone seen in A was a control with no voltage applied. Photographs B, C, and D show a bone stimulated with 15 v, 30 v, and 50 v respectively.

Table 1.--Data for calculated displacement of adult bone surface*

Voltage	Observation**	Number of Fringes per Adult Sample				
		1	2	3	4	5
100 v	Horizontal	0.5	0.7	0.9	0.5	0.5
	45 Degrees	0.5	0.3	0.9	0.5	0.5
	Vertical	0.3	0.1	0.1	0.5	0.0
	120 Degrees	0.3	0.2	0.2	0.5	0.0
150 v	Horizontal	3.0	4.0	3.0	3.0	5.0
	45 Degrees	4.0	2.0	3.0	4.0	4.0
	Vertical	1.0	1.0	0.0	0.0	2.0
	120 Degrees	1.0	1.0	1.0	2.0	1.0
200 v	Horizontal	8.0	7.0	8.0	6.0	7.0
	45 Degrees	4.0	4.0	5.0	4.0	3.0
	Vertical	2.0	2.0	1.0	3.0	2.0
	120 Degree	4.0	1.0	3.0	0.0	3.0

*Duration of voltage application: 30 seconds.

**The four directions of observation (P_1 to P_2), as well as the number and direction of fringes which pass through the site measured on the bone surface, are included in this table for each voltage applied.

Table 2.--Data for calculated displacement of juvenile bone surface*

Voltage	Observation**	Number of Fringes per Juvenile Sample				
		1	2	3	4	5
15 v	Horizontal	0.5	0.4	0.5	0.5	0.7
	45 Degrees	0.3	0.3	0.5	0.5	0.2
	Vertical	-0.2	0.0	0.2	0.2	-0.5
	120 Degrees	0.5	0.2	1.0	0.0	0.2
30 v	Horizontal	4.0	3.0	4.0	3.0	3.4
	45 Degrees	5.0	3.5	4.0	3.0	2.0
	Vertical	0.0	-1.0	0.0	-2.0	-1.0
	120 Degrees	2.0	2.0	3.0	1.0	3.0
50 v	Horizontal	6.0	8.0	6.5	9.0	6.0
	45 Degrees	4.0	5.0	4.0	5.0	4.0
	Vertical	-3.0	-3.0	-3.0	-3.0	-2.5
	120 Degrees	2.0	2.0	2.0	3.0	2.0

*Duration of voltage application: 20 seconds.

**The four directions of observation (P_1 to P_2), as well as the number and direction of fringes which pass through the site measured on the bone surface, are included in this table for each voltage applied.

observed on the reconstructed surface when changing the direction of observation through the hologram from P_1 to P_2 . It was observed that when the electrical polarity was reversed, the fringes moved in opposite directions with respect to P_1 to P_2 , indicating the effect was electrical rather than thermal.

A mathematical interpretation of interference fringes was used to determine the magnitude and direction of bone displacement in response to an applied voltage. Equation 1 represents the basic equation used to relate surface displacement on the reconstructed image to the observed fringe shifts when the angle of observation is changed.

$$(1) \quad \Delta \vec{r} \cdot \Delta \vec{n} = \pm k \lambda$$

$\Delta \vec{r}$ represents the surface displacement vector.

$\Delta \vec{n}$ represents the difference in the unit vector ($\Delta \vec{n} = \vec{n}_2 - \vec{n}_1$) corresponding to a change in the direction of observation.

$\pm k$ is the number of fringes passing the point on the surface being observed in moving from P_1 to P_2 with the + or - sign indicating the direction of fringe movement.

λ is the wavelength of the laser (632.8 nm).

The components of the unit vector are:

$$\begin{aligned} \text{for } P_1 \quad n_{1x} &= n \cos \theta_1 \\ n_{1y} &= n \sin \theta_1 \cos \alpha_1 \\ n_{1z} &= n \sin \theta_1 \sin \alpha_1 \end{aligned}$$

$$\begin{aligned} \text{for } P_2 \quad n_{2x} &= n \cos \theta_2 \\ n_{2y} &= n \sin \theta_2 \cos \alpha_2 \\ n_{2z} &= n \sin \theta_2 \sin \alpha_2 \end{aligned}$$

where $n = 1$

The above was repeated for each of the four observations (horizontal, 45 degrees, vertical, and 120 degrees; see Appendix II for calculations). Δn , the change in the unit vector, n is given by:

$$\begin{aligned} \Delta \vec{n}_x &= \vec{n}_{2x} - \vec{n}_{1x} \\ \Delta \vec{n}_y &= \vec{n}_{2y} - \vec{n}_{1y} \\ \Delta \vec{n}_z &= \vec{n}_{2z} - \vec{n}_{1z} \end{aligned}$$

The components of $\Delta \vec{n}$ for each observation comprise the elements of a matrix which, along with $k\lambda$, are used to estimate the displacement vector components. A tabulation of results for the various Δn and $k\lambda$ are given in Tables 3, 4, 5, and 6 for the observed surface displacement of the bones.

The fringe shifts on the plastic bar moved from P_2 to P_1 when displaced; likewise, the bone samples measured exhibited the same direction of fringe motion. However, the plastic bar was actually moved in the direction opposite

Table 3a.--Unit vector components of adult bone surface

Observation	Vector Components		
	Δn_x^*	Δn_y^*	Δn_z^*
Horizontal	-0.014	0.770	0.000
45 Degrees	-0.070	0.695	0.695
Vertical	-0.075	0.000	1.268
120 Degrees	-0.102	0.580	0.557

Table 3b.--Unit vector components of juvenile bone surface

Observation	Vector Components		
	Δn_x^{**}	Δn_y^{**}	Δn_z^{**}
Horizontal	-0.019	0.893	0.000
45 Degrees	-0.093	0.475	0.475
Vertical	-0.102	0.000	0.311
120 Degrees	-0.133	0.373	0.640

*The Δn_x , Δn_y , and Δn_z are the same for samples stimulated with 100 v, 150 v, and 200 v.

**The Δn_x , Δn_y , and Δn_z are the same for samples stimulated with 15 v, 30 v, and 50 v.

Table 4.--Calculated data for displacement of adult bone surface

Voltage	Vector	Displacement Vector Components				
		Sample Number				
		1	2	3	4	5
100 v	r_1	3.3	5.1	9.6	0.8	7.1
	r_2	0.7	0.9	1.4	0.6	0.9
	r_3	0.4	0.3	0.7	0.4	0.4
	\vec{r}_{yz}^*	0.8	0.9	1.6	0.7	1.0
150 v	r_1	34.2	35.6	24.2	10.2	59.8
	r_2	5.1	5.1	4.7	4.9	7.3
	r_3	3.0	2.6	1.6	0.9	5.0
	\vec{r}_{yz}^*	5.9	5.7	4.9	5.0	8.8
200 v	r_1	34.8	79.6	51.6	93.7	38.8
	r_2	9.2	9.5	10.4	8.7	8.0
	r_3	3.0	6.0	3.5	7.6	3.2
	\vec{r}_{yz}^*	9.7	11.2	11.0	11.5	8.6

*The computed displacement value for each experiment in microns.

Table 5.--Calculated data for displacement of juvenile bone surface

Voltage	Vector	Displacement Vector Components				
		Sample Number				
		1	2	3	4	5
15 v	r_1	6.1	9.3	1.2	0.2	9.3
	r_2	0.7	0.5	0.5	0.5	1.0
	r_3	1.5	3.7	1.2	0.8	1.5
	\vec{r}_{yz}^*	2.1	3.8	1.7	0.9	2.1
30 v	r_1	25.3	41.5	21.7	54.9	32.5
	r_2	5.3	4.3	5.0	4.7	4.1
	r_3	7.2	10.0	6.8	11.1	8.0
	\vec{r}_{yz}^*	8.9	10.9	8.4	12.0	8.9
50 v	r_1	71.1	66.7	67.9	65.0	59.9
	r_2	8.3	10.5	8.7	11.5	8.0
	r_3	13.4	11.7	12.4	11.6	11.4
	\vec{r}_{yz}^*	15.8	15.7	15.1	16.3	13.9

*The computed displacement value for each experiment in microns.

Table 6.--Average values for adult and juvenile bone displacement*

Voltage	Adult Displacement	Voltage	Juvenile Displacement
100 v	1.0 \pm 0.3	15 v	2.1 \pm 0.7
150 v	6.1 \pm 1.1	30 v	9.8 \pm 1.3
200 v	10.4 \pm 1.2	50 v	15.4 \pm 0.8

*The average values for bone displacement (in microns) and standard deviation are listed for each voltage increment used.

to fringe movement. Hence, it was determined that the actual direction of bone displacement was in the P_2 to P_1 direction in the yz -planes. The x -component of $\Delta \vec{r}$ had a large uncertainty with regard to bone displacement since all the fringe observation points were in the yz -planes; thus it was omitted.

CHAPTER IV

CONCLUSIONS

The magnitude and direction of bone displacement in response to electrical stimulation was assessed for adult and juvenile tibias. The juvenile bone samples exhibited a greater degree of displacement at significantly lower voltages than the adult samples. This phenomenon supports the idea that collagen is the source of the piezoelectric effect in bone since the juvenile bones have a proportionately higher ratio of collagen to inorganic salts than the adult bones. In all cases the amount of bone displacement increased when the sample was subjected to a larger voltage. The direction of bone displacement is dependent on the arrangement of the electrodes since the displacement direction was reversed when the polarity was reversed. This experiment revealed the ordered nature of the piezoelectric effect in bone; that is: 1) an electrical stimulation produces a slight change in the surface position of the bone; 2) the resulting change is dependent on the morphological state of the bone (mature or immature); 3) an increase in the voltage results in an increase in surface displacement; 4) the displacement direction is dependent upon electrical polarity.

This research demonstrates that a short-term applied voltage temporarily realigns the bone surface, presumably by reorienting the intramolecular bonds of collagen. It would be interesting to investigate the effects of long term bone displacement in response to an applied voltage. In such an investigation it would be useful to assess the accompanying change in the external and internal architecture of the bone. An investigation of this type could eventually lead to a clinical application whereby a desired structural change in the bone's morphology could be accomplished.

APPENDIX I

Programmed Solution for a Set

of

Linearly Independent Nonhomogeneous Equations

```
DIM A(3,3), B(3), R(3), W(3,3), X(4,3), Y(4), Z(3,4)
FOR K=1 TO 4
PRINT "ENTER ELEMENTS OF ROW "K;" FOR MATRIX X(I,J)";
INPUT X(K,1), X(K,2), X(K,3)
NEXT K
PRINT
PRINT
PRINT "MATRIX X"
MAT PRINT X
FOR K=1 TO 4
PRINT "ENTER ELEMENT #K;" FOR THE COLUMN VECTOR Y(I)";
INPUT Y(K)
NEXT K
PRINT "MATRIX Y"
MAT PRINT Y
MAT X=TRN (X)
MAT W=Z*X
MAT A=INV(W)
MAT B=Z*Y
MAT R=A*B
PRINT "R1="R(1)
PRINT "R2="R(2)
PRINT "R3="R(3)
PRINT
PRINT "PRINT OUT EXTRA MATRICES? 1=YES 0=NO"
INPUT P
IF P=0, THEN 381
```

```
PRINT "MATRIX A"  
MAT PRINT A  
PRINT  
PRINT  
PRINT "MATRIX B"  
MAT PRINT B  
PRINT  
PRINT  
PRINT "MATRIX W"  
MAT PRINT W  
PRINT  
PRINT  
PRINT "MATRIX Z"  
MAT PRINT Z  
PRING "WANT TO DO IT AGAIN? 1=YES 0=NO"  
INPUT Q  
IF Q=1, THEN 110  
END
```

APPENDIX II

Calculations for Adult and Juvenile
Vector Components
for each Observation

CALCULATIONS FOR THE ADULT VECTOR COMPONENTS

A. Horizontal Components of Δn_x , Δn_y , and Δn_z

$$\underline{\Delta n_x}$$

$$\begin{aligned} n_{1x} &= n \cos \theta_1 \\ &= \frac{4.5 \text{ cm}}{11.3 \text{ cm}} \\ &= 0.929 \end{aligned}$$

$$\begin{aligned} n_{2x} &= n \cos \theta_2 \\ &= \frac{5.0 \text{ cm}}{11.3 \text{ cm}} \\ &= 0.915 \end{aligned}$$

$$\begin{aligned} \Delta n_x &= n_{2x} - n_{1x} \\ &= 0.915 - 0.929 \\ &= -0.014 \end{aligned}$$

$$\underline{\Delta n_y}$$

$$\begin{aligned} n_{1y} &= n \sin \theta_1 \cos \alpha_1 \\ &= \frac{4.5 \text{ cm}}{11.3 \text{ cm}} (-1) \\ &= -0.37 \end{aligned}$$

$$\begin{aligned} n_{2y} &= n \sin \theta_2 \cos \alpha_x \\ &= \frac{5.0 \text{ cm}}{11.3 \text{ cm}} (1) \\ &= 0.40 \end{aligned}$$

$$\begin{aligned} \Delta n_y &= n_{2y} - n_{1y} \\ &= 0.40 - (-0.37) \\ &= 0.770 \end{aligned}$$

$$\underline{\Delta n_z}$$

$$\begin{aligned} n_{1z} &= n \sin \theta_1 \sin \alpha_1 \\ &= \frac{5.0 \text{ cm}}{11.3 \text{ cm}} (0) \\ &= 0.0 \end{aligned}$$

$$\begin{aligned} n_{2z} &= n \sin \theta_2 \sin \alpha_2 \\ &= \frac{4.5 \text{ cm}}{11.3 \text{ cm}} (0) \\ &= 0.0 \end{aligned}$$

$$\begin{aligned} \Delta n_z &= n_{2z} - n_{1z} \\ &= 0.0 - 0.0 \\ &= 0.0 \end{aligned}$$

B. 45 Degree Components of Δn_x , Δn_y , and Δn_z

Δn_x

$$\begin{aligned}n_{1x} &= n \cos \theta_1 \\ &= \frac{2.0 \text{ cm}}{11.3 \text{ cm}} \\ &= 0.985\end{aligned}$$

$$\begin{aligned}n_{2x} &= n \cos \theta_2 \\ &= \frac{5.0 \text{ cm}}{11.3 \text{ cm}} \\ &= 0.915\end{aligned}$$

$$\begin{aligned}\Delta n_x &= n_{2x} - n_{1x} \\ &= 0.915 - 0.985 \\ &= 0.07\end{aligned}$$

Δn_y

$$\begin{aligned}n_{1y} &= n \sin \theta_1 \cos \alpha_1 \\ &= \frac{2.0 \text{ cm}}{11.3 \text{ cm}} (-.707) \\ &= -0.123\end{aligned}$$

$$\begin{aligned}n_{2y} &= n \sin \theta_2 \cos \alpha_2 \\ &= \frac{5.0 \text{ cm}}{11.3 \text{ cm}} (.707) \\ &= 0.572\end{aligned}$$

$$\begin{aligned}\Delta n_y &= n_{2y} - n_{1y} \\ &= 0.572 - (-0.123) \\ &= 0.695\end{aligned}$$

Δn_z

$$\begin{aligned}n_{1z} &= n \sin \theta_1 \sin \alpha_1 \\ &= \frac{2.0 \text{ cm}}{11.3 \text{ cm}} (-.707) \\ &= -0.123\end{aligned}$$

$$\begin{aligned}n_{2z} &= n \sin \theta_2 \sin \alpha_2 \\ &= \frac{5.0 \text{ cm}}{11.3 \text{ cm}} (.707) \\ &= 0.572\end{aligned}$$

$$\begin{aligned}\Delta n_z &= n_{2z} - n_{1z} \\ &= 0.572 - (-0.123) \\ &= 0.695\end{aligned}$$

C. Vertical Components of Δn_x , Δn_y , and Δn_z

$$\underline{\Delta n_x}$$

$$\begin{aligned}n_{1x} &= n \cos \theta_1 \\ &= \frac{1.5 \text{ cm}}{11.3 \text{ cm}} \\ &= 0.99\end{aligned}$$

$$\begin{aligned}n_{2x} &= n \cos \theta_2 \\ &= \frac{5.0 \text{ cm}}{11.3 \text{ cm}} \\ &= 0.915\end{aligned}$$

$$\begin{aligned}\Delta n_x &= n_{2x} - n_{1x} \\ &= 0.915 - 0.99 \\ &= -0.075\end{aligned}$$

$$\underline{\Delta n_y}$$

$$\begin{aligned}n_{1y} &= n \sin \theta_1 \cos \alpha_1 \\ &= \frac{1.5 \text{ cm}}{11.3 \text{ cm}} (0) \\ &= 0.0\end{aligned}$$

$$\begin{aligned}n_{2y} &= n \sin \theta_2 \cos \alpha_2 \\ &= \frac{5.0 \text{ cm}}{11.3 \text{ cm}} (1) \\ &= 0.0\end{aligned}$$

$$\begin{aligned}\Delta n_y &= n_{2y} - n_{1y} \\ &= 0.0 - 0.0 \\ &= 0.0\end{aligned}$$

$$\underline{\Delta n_z}$$

$$\begin{aligned}n_{1z} &= n \sin \theta_1 \sin \alpha_1 \\ &= \frac{1.5 \text{ cm}}{11.3 \text{ cm}} (1) \\ &= 0.680\end{aligned}$$

$$\begin{aligned}n_{2z} &= n \sin \theta_2 \sin \alpha_2 \\ &= \frac{5.0 \text{ cm}}{11.3 \text{ cm}} (1) \\ &= 0.202\end{aligned}$$

$$\begin{aligned}\Delta n_z &= n_{2z} - n_{1z} \\ &= 0.202 - (-0.68) \\ &= 0.802\end{aligned}$$

D. 120 Degree Components of Δn_x , Δn_y , and Δn_z

$$\underline{\Delta n_x}$$

$$\begin{aligned} n_{1x} &= n \cos \theta_1 \\ &= \frac{2.0 \text{ cm}}{11.3 \text{ cm}} \\ &= 0.985 \end{aligned}$$

$$\begin{aligned} n_{2x} &= n \cos \theta_2 \\ &= \frac{6.0 \text{ cm}}{11.3 \text{ cm}} \\ &= 0.883 \end{aligned}$$

$$\begin{aligned} \Delta n_x &= n_{2x} - n_{1x} \\ &= .0883 - 0.985 \\ &= -0.102 \end{aligned}$$

$$\underline{\Delta n_y}$$

$$\begin{aligned} n_{1y} &= n \sin \theta_1 \cos \alpha_1 \\ &= \frac{2.0 \text{ cm}}{11.3 \text{ cm}} (-.5) \\ &= -0.349 \end{aligned}$$

$$\begin{aligned} n_{2y} &= n \sin \theta_2 \sin \alpha_2 \\ &= \frac{6.0 \text{ cm}}{11.3 \text{ cm}} (.5) \\ &= 0.234 \end{aligned}$$

$$\begin{aligned} \Delta n_y &= n_{2y} - n_{1y} \\ &= 0.234 - (-0.349) \\ &= 0.583 \end{aligned}$$

$$\underline{\Delta n_z}$$

$$\begin{aligned} n_{1z} &= n \sin \theta_1 \sin \alpha_1 \\ &= \frac{2.0 \text{ cm}}{11.3 \text{ cm}} (-0.866) \\ &= 0.151 \end{aligned}$$

$$\begin{aligned} n_{2z} &= n \sin \theta_2 \sin \alpha_2 \\ &= \frac{6.0 \text{ cm}}{11.3 \text{ cm}} (0.866) \\ &= 0.406 \end{aligned}$$

$$\begin{aligned} \Delta n_z &= n_{2z} - n_{1z} \\ &= 0.406 - (-0.151) \\ &= 0.557 \end{aligned}$$

CALCULATIONS FOR THE JUVENILE VECTOR COMPONENTS

A. Horizontal Components of Δn_x , Δn_y , and Δn_z

Δn_x

$$\begin{aligned} n_{1x} &= n \cos \theta_1 \\ &= \frac{4.5 \text{ cm}}{9.5 \text{ cm}} \\ &= 0.904 \end{aligned}$$

$$\begin{aligned} n_{2x} &= n \cos \theta_2 \\ &= \frac{5.0 \text{ cm}}{9.5 \text{ cm}} \\ &= 0.885 \end{aligned}$$

$$\begin{aligned} \Delta n_x &= n_{2x} - n_{1x} \\ &= 0.885 - 0.904 \\ &= -0.019 \end{aligned}$$

Δn_y

$$\begin{aligned} n_{1y} &= n \sin \theta_1 \cos \alpha_1 \\ &= \frac{5.0 \text{ cm}}{9.5 \text{ cm}} (1) \\ &= 0.465 \end{aligned}$$

$$\begin{aligned} n_{2y} &= n \sin \theta_2 \cos \alpha_2 \\ &= \frac{4.5 \text{ cm}}{9.5 \text{ cm}} (-1) \\ &= 0.428 \end{aligned}$$

$$\begin{aligned} \Delta n_y &= n_{2y} - n_{1y} \\ &= 0.428 - (-0.465) \\ &= 0.893 \end{aligned}$$

Δn_z

$$\begin{aligned} n_{1z} &= n \sin \theta_1 \sin \alpha_1 \\ &= \frac{5.0 \text{ cm}}{9.5 \text{ cm}} (0) \\ &= 0.0 \end{aligned}$$

$$\begin{aligned} n_{2z} &= n \sin \theta_2 \sin \alpha_2 \\ &= \frac{4.5 \text{ cm}}{9.5 \text{ cm}} (0) \\ &= 0.0 \end{aligned}$$

$$\begin{aligned} \Delta n_z &= n_{2z} - n_{1z} \\ &= 0.0 - 0.0 \\ &= 0.0 \end{aligned}$$

B. 45 Degree Components of Δn_x , Δn_y , and Δn_z

Δn_x

$$\begin{aligned}n_{1x} &= n \cos \theta_1 \\ &= \frac{2.0 \text{ cm}}{9.5 \text{ cm}} \\ &= 0.978\end{aligned}$$

$$\begin{aligned}n_{2x} &= n \cos \theta_2 \\ &= \frac{5.0 \text{ cm}}{9.5 \text{ cm}} \\ &= 0.885\end{aligned}$$

$$\begin{aligned}\Delta n_x &= n_{2x} - n_{1x} \\ &= 0.885 - 0.978 \\ &= -0.093\end{aligned}$$

Δn_y

$$\begin{aligned}n_{1y} &= n \sin \theta_1 \cos \alpha_1 \\ &= \frac{2.0 \text{ cm}}{9.5 \text{ cm}} (-.707) \\ &= -0.146\end{aligned}$$

$$\begin{aligned}n_{2y} &= n \sin \theta_2 \cos \alpha_2 \\ &= \frac{5.0 \text{ cm}}{9.5 \text{ cm}} (.707) \\ &= 0.329\end{aligned}$$

$$\begin{aligned}\Delta n_y &= n_{2y} - n_{1y} \\ &= 0.329 - (-0.146) \\ &= 0.475\end{aligned}$$

Δn_z

$$\begin{aligned}n_{1z} &= n \sin \theta_1 \sin \alpha_1 \\ &= \frac{2.0 \text{ cm}}{9.5 \text{ cm}} (-.707) \\ &= -0.146\end{aligned}$$

$$\begin{aligned}n_{2z} &= n \sin \theta_2 \sin \alpha_2 \\ &= \frac{5.0 \text{ cm}}{9.5 \text{ cm}} (.707) \\ &= 0.329\end{aligned}$$

$$\begin{aligned}\Delta n_z &= n_{2z} - n_{1z} \\ &= 0.329 - (-0.146) \\ &= 0.475\end{aligned}$$

C. Vertical Components of Δn_x , Δn_y , and Δn_z

$$\underline{\Delta n_x}$$

$$\begin{aligned} n_{1x} &= n \cos \theta_1 \\ &= \frac{1.5 \text{ cm}}{9.5 \text{ cm}} \\ &= 0.987 \end{aligned}$$

$$\begin{aligned} n_{2x} &= n \cos \theta_2 \\ &= \frac{5.0 \text{ cm}}{9.5 \text{ cm}} \\ &= 0.855 \end{aligned}$$

$$\begin{aligned} \Delta n_x &= n_{2x} - n_{1x} \\ &= 0.855 - 0.987 \\ &= -0.102 \end{aligned}$$

$$\underline{\Delta n_y}$$

$$\begin{aligned} n_{1y} &= n \sin \theta_1 \cos \alpha_1 \\ &= \frac{1.5 \text{ cm}}{9.5 \text{ cm}} (0) \\ &= 0.0 \end{aligned}$$

$$\begin{aligned} n_{2y} &= n \sin \theta_2 \cos \alpha_2 \\ &= \frac{5.0 \text{ cm}}{9.5} (0) \\ &= 0.0 \end{aligned}$$

$$\begin{aligned} \Delta n_y &= n_{2y} - n_{1y} \\ &= 0.0 - 0.0 \\ &= 0.0 \end{aligned}$$

$$\underline{\Delta n_z}$$

$$\begin{aligned} n_{1z} &= n \sin \theta_1 \sin \alpha_1 \\ &= \frac{1.5 \text{ cm}}{9.5 \text{ cm}} (1) \\ &= -0.078 \end{aligned}$$

$$\begin{aligned} n_{2z} &= n \sin \theta_2 \sin \alpha_2 \\ &= \frac{5.0 \text{ cm}}{9.5 \text{ cm}} (1) \\ &= 0.233 \end{aligned}$$

$$\begin{aligned} \Delta n_z &= n_{2z} - n_{1z} \\ &= 0.233 - (-0.078) \\ &= 0.311 \end{aligned}$$

D. 120 Degree Components of Δn_x , Δn_y , and Δn_z

Δn_x

$$\begin{aligned}n_{1x} &= n \cos \theta_1 \\ &= \frac{2.0 \text{ cm}}{9.5 \text{ cm}} \\ &= 0.978\end{aligned}$$

$$\begin{aligned}n_{2x} &= n \cos \theta_2 \\ &= \frac{6.0 \text{ cm}}{9.5 \text{ cm}} \\ &= 0.845\end{aligned}$$

$$\begin{aligned}\Delta n_x &= n_{2x} - n_{1x} \\ &= 0.845 - 0.978 \\ &= -0.133\end{aligned}$$

Δn_y

$$\begin{aligned}n_{1y} &= n \sin \theta_1 \cos \alpha_1 \\ &= \frac{2.0 \text{ cm}}{9.5 \text{ cm}} (-.5) \\ &= -0.103\end{aligned}$$

$$\begin{aligned}n_{2y} &= n \sin \theta_2 \sin \alpha_2 \\ &= \frac{6.0 \text{ cm}}{9.5 \text{ cm}} (.5) \\ &= 0.27\end{aligned}$$

$$\begin{aligned}\Delta n_y &= n_{2y} - n_{1y} \\ &= 0.27 - (-0.103) \\ &= 0.373\end{aligned}$$

Δn_z

$$\begin{aligned}n_{1z} &= n \sin \theta_1 \sin \alpha_1 \\ &= \frac{2.0 \text{ cm}}{9.5 \text{ cm}} (-.866) \\ &= -0.178\end{aligned}$$

$$\begin{aligned}n_{2z} &= n \sin \theta_2 \sin \alpha_2 \\ &= \frac{6.0 \text{ cm}}{9.5 \text{ cm}} (.866) \\ &= 0.462\end{aligned}$$

$$\begin{aligned}\Delta n_z &= n_{2z} - n_{1z} \\ &= 0.462 - (-0.178) \\ &= 0.640\end{aligned}$$

REFERENCES

- Aleksandrov, E. B. and A. M. Bonch-Bruevich. 1967. Investigations of surface strains by the hologram technique. Soviet Tech. Phys. XII:258-265.
- Bassett, C. A. L., R. J. Pawluk, and R. D. Becker. 1964. Effects of electric current on bone in vivo. Nature 204:652.
- Bassett, C. A. L. 1968. Biological significance of piezoelectricity. Calcified Tissue Research I:253.
- Bourne, G. H. 1971. The Biochemistry and Physiology of Bone. Vol. III. Academic Press, New York and London. pp. 10-12.
- Castillo, T. 1974. Holographic Study of the Electrical Response of Bone. M. S. Thesis. Southwest Texas State University.
- Cathey, T. W. 1974. Optical Information Processing and Holography. John Wiley and Sons, Inc. New York, New York. p. 324.
- Fukada, E. and I. Yasuda. 1957. On the piezoelectric effect of bone. J. of Phys. Soc. Japan. 10:1158-1162.
- Fukada, E. and I. Yasuda. 1964. Piezoelectric effects in collagen. J. of Applied Phys. 3:117.
- Harris, W. 1977. Differential response to electrical stimulation: A distinction between "induced osteogenesis in intact tibiae and effects on fresh fracture defects in radii. J. of Clinical Orthopedic. I:31.
- Norton, L. 1977. Epiphyseal cartilage cAMP changes produced by electrical and mechanical perturbations. J. of Clinical Orthopedics. I:50.
- Williams, W. S. 1974. Sources of piezoelectricity in tendon and bone. CRC Critical Reviews in Bioengineering. 2(1):95-96.

Williams, W. S. 1974. Electrical modification of disuse osteoporosis. *Calcified Tissue Research*. 18(2): 111.

White, D. 1976. Frequency Dependence of the Electrical Response of Bone. M. S. Thesis. Southwest Texas State University.